Dark field X-ray microscopy for studies of recrystallization

Ahl, Sonja Rosenlund; Simons, Hugh; Jakobsen, Anders Clemen; Zhang, Yubin; Stöhr, Frederik; Juul Jensen, Dorte; Poulsen, Henning Friis

Published in:
I O P Conference Series: Materials Science and Engineering

Link to article, DOI:
10.1088/1757-899X/89/1/012016

Publication date:
2015

Document Version
Publisher's PDF, also known as Version of record

Dark field X-ray microscopy for studies of recrystallization

2015 IOP Conf. Ser.: Mater. Sci. Eng. 89 012016

(http://iopscience.iop.org/1757-899X/89/1/012016)

Dark field X-ray microscopy for studies of recrystallization

S R Ahl[1], H Simons[1,2], A C Jakobsen[1], Y B Zhang[3], F Stöhr[4], D Juul Jensen[3] and H F Poulsen[1]

[1] Department of Physics, Technical University of Denmark, 2800 Kgs. Lyngby, Denmark
[2] European Synchrotron Radiation Facility, CS 40220, 38043 Grenoble Cedex 9, France
[3] Department of Wind Energy, Technical University of Denmark, 4000 Roskilde, Denmark
[4] DTU Danchip, Technical University of Denmark, 2800 Kgs. Lyngby, Denmark

E-mail: sroh@fysik.dtu.dk

Abstract. We present the recently developed technique of Dark Field X-Ray Microscopy that utilizes the diffraction of hard X-rays from individual grains or subgrains at the (sub)micrometre-scale embedded within mm-sized samples. By magnifying the diffracted signal, 3D mapping of orientations and strains inside the selected grain is performed with an angular resolution of 0.005° and a spatial resolution of 200 nm. Furthermore, the speed of the measurements at high-intensity synchrotron facilities allows for fast non-destructive *in situ* determination of structural changes induced by annealing or other external influences. The capabilities of Dark Field X-Ray Microscopy are illustrated by examples from an ongoing study of recrystallization of 50% cold-rolled Al1050 specimens.

1. Introduction

Current methods for microstructural mapping such as Electron Back-Scatter Diffraction (EBSD [1]) and standard Transmission Electron Microscopy (TEM [2]) are inherently two-dimensional (2D) and can therefore not directly map the microstructure of bulk materials. X-ray techniques such as 3D X-Ray Diffraction (3DXRD [3]), Diffraction Contrast Tomography (DCT [4]), and 3D Polychromatic X-Ray Microscopy [5] can provide 3D maps of polycrystals, but cannot resolve nano-scale features. Recently, Dark Field X-Ray Microscopy (DFXRM) demonstrated the ability to measure 3D maps of orientations within individual deformed grains with 300 nm spatial resolution [6]. Importantly, this non-destructive technique offers the unique possibility of *in situ* studies of 3D structural changes during recovery and recrystallization processes in polycrystalline metals. In addition to sub-micrometre spatial resolution, the remarkable angular resolution, better than 0.005°, allows for mapping of internal structures with very small angular differences - orders of magnitude less than those resolvable by other means.

With this new tool it will potentially be possible to map not only the recrystallized grains but also the deformed structures surrounding the grain. Thus we will now be able to study individual new grains, their possible internal structure of very low angle boundaries, and their growth into the deformed material, resolving individual dislocations and dislocation boundaries in the deformed material. Strain fields at grain boundaries and around single dislocations may be mapped, and we may be able to obtain new insight into the internal structure of partly recrystallized metals as well as the processes occurring during recovery. For instance, it has

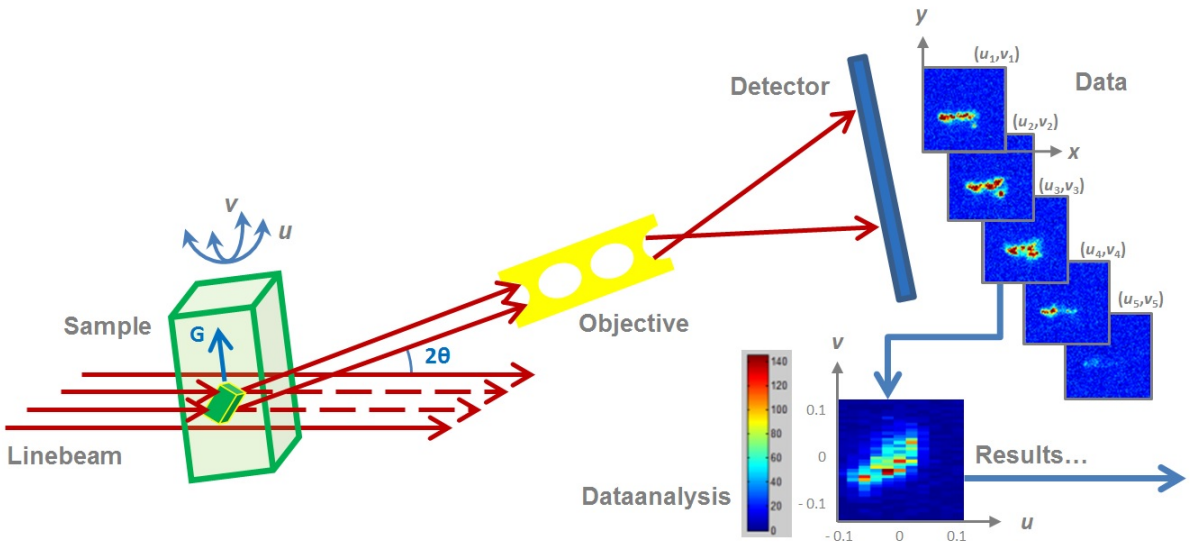

Figure 1. Sketch of the experimental setup of DFXRM and data acquisition. A line beam illuminates a plane of the polycrystalline sample. The diffracted signal is magnified by the objective and direct space images are collected. The orientation of the scattering vector **G** is varied by tilting the sample slightly in the two perpendicular angles u and v. From the raw images a 2D rocking curve for each pixel is constructed and further analysis of the internal structure of the sample carried out.

been hypothesized that when subgrains in deformed material merge during recovery, their lattices rotate towards a common orientation [7], yet this rotation has not been directly observed. With DFXRM, we are able to resolve very small angular changes in lattice orientation, potentially enabling direct observations of this phenomenon. Furthermore, grain boundaries may be resolved with sub-micrometre resolution through a series of annealing steps, allowing us to study grain coarsening in a fully recrystallized sample.

In this paper we outline the DFXRM technique and describe our current instrumentation, which is an *ad hoc* setup being developed in collaboration between the Technical University of Denmark (DTU) and the European Synchrotron Radiation Facility (ESRF) in France. To illustrate the capabilities of DFXRM we present preliminary data from an ongoing study of the recrystallization of aluminium. The spatial resolution of the data presented is better than 200 nm and angular differences of 0.005° are resolved. We demonstrate that inside micrometre-sized recrystallizing grains in the present sample there exist very low angle boundaries with angular differences of less than 0.1°.

2. Instrument description

The defining feature of DFXRM is that it magnifies the X-rays scattered by a crystalline material through Bragg diffraction. For crystal lattice planes separated by a distance d, X-rays of wavelength λ will be diffracted through the angle 2θ according to Braggs law: $\lambda = 2d\sin\theta$. DFXRM, see Figure 1, utilizes hard X-rays with energies of at least 15 keV, which are necessary

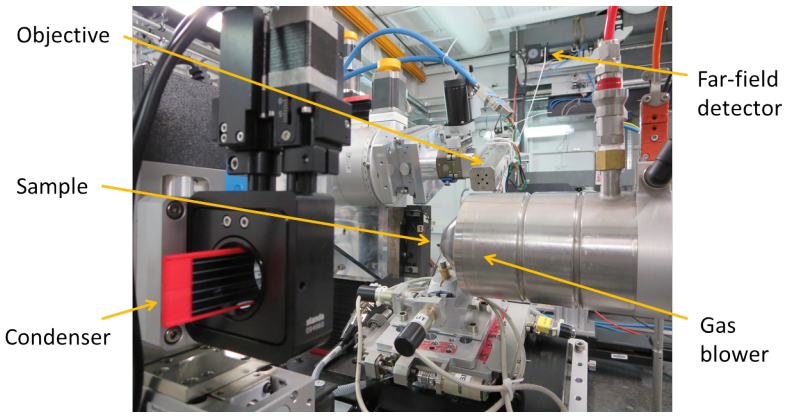

Figure 2. Beamline ID06. The instrument is set up for the experiment described in the case study below. A gas blower is mounted for annealing studies.

to penetrate into the bulk of large (typically millimeter-sized) samples. To ensure that sampling times are commensurate with the material dynamics, DFXRM uses intense x-rays from the high-brilliance x-ray source of the ESRF. Specifically, the instrument is located at beamline ID066, see Figure 2.

When the sample is properly aligned in the beam, a grain inside the sample with a clear diffraction spot is selected on a near-field detector positioned 1-5 cm away from the sample. The diffracted signal is then magnified through an objective onto a far-field detector several meters away, giving a direct space image of the diffracted signal from the illuminated part of the sample at this particular sample orientation.

While the concept of imaging the diffracted intensity is common with Diffraction Topography [8], it is the additional inclusion of the imaging objective that makes DFXRM unique in its angular and spatial resolution. Furthermore, we are currently working towards a setup with variable magnification, to give the opportunity of zooming in and out. With this a spatial resolution of 50 nm should be within reach. The objective is a compound refractive lens [9] that consists of a series of individual refractive X-ray lenses that combine to give a practically manageable focal length, typically 20-40 cm. Thus, the objective can be positioned along the diffracted beam such that it forms a spatial image on the far-field detector. The contrast in this image arises from the diffraction process, meaning that local changes in d-spacing and orientation in the sample are visible as intensity gradients in the image. Due to the absorbing nature of the X-ray objective, the numerical aperture (i.e. angular acceptance) of the system is very small (0.1°). This implies that we observe the spatial distribution of regions with a specific orientation and d-spacing of the lattice planes.

Since the instrument only images a very small range of orientations and lattice spacings, mapping samples with any orientation and strain distributions requires taking multiple exposures while scanning the sample and/or the axis of the diffracted beam and recombining these images into a composite. For example, by tilting the sample slightly through the two perpendicular angles (u, v), see Figure 1, the internal deviation of the lattice plane orientation is mapped for the illuminated region of the sample. Specifically, raw images for a 2D-set of perpendicular tilt-angles are collected and from this set the measured small section of the full pole figure is extracted as a 2D rocking curve for each direct space coordinate, see Figure 3 and 5. The (u, v)-values for the maximum intensity is determined from a Gaussian moment fit and this information is collected in a colour-coded direct space image, showing the distribution of lattice orientations, see Figure 4(c). Similarly, elastic strain (i.e. the variations in lattice spacing) may

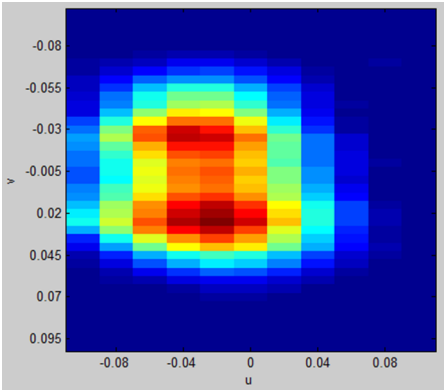

Figure 3. Summed 2D rocking curve. The summed intensity of the image for each value of the tilts (u, v) is mapped in arbitrary units where red indicates large intensity and blue is small.

be mapped through consecutive scans in which the sample is kept stationary and the objective and detector are moved together in a narrow 2θ-range around the nominal diffraction angle for the unstrained lattice.

The image visible in the detector constitutes a 2D projection through the illuminated volume of the sample. Therefore, 3D mapping with high resolution must be performed layer-by-layer and a small vertical dimension of the beam is required for the detector image to represent a single slice of the sample. This is achieved by condensing the incoming beam to a line beam. Then a 3D volume can be mapped by repeating the above procedure while moving the sample vertically in steps. The slices are then combined layer-by-layer to a 3D image during postprocessing.

Annealing, deformation, and other transformative processes may be introduced and measurements may be performed stop-go, to map the structural changes during the processes. Repeating the measurement after external stimuli provides information on the induced structural changes in 3D.

3. Case study: Partly recrystallized Al1050

Here we present preliminary results from an ongoing study of recrystallization of aluminium to illustrate the capabilities of DFXRM.

3.1. Sample

A sample of aluminium Al1050 cold-rolled to 50% reduction in thickness was cut into a rod of 300×300 μm^2 cross-section perpendicular to the rolling direction (RD) and heat-treated for 50 minutes at 325°C (almost 50% recrystallized). The rod was aligned in the line beam and tilted to $\theta = 11.8^{\circ}$ to look at the (200)-reflection ($d = 4.04$ Å) with the lattice plane normal along the RD. A recrystallizing grain of $15 \times 20 \times 20$ μm^3 in size was located within the bulk of the sample. It is presumed, but not investigated, that the grain is surrounded by deformed material.

3.2. Experimental

The DFXRM instrument is located at the beamline ID06 at the ESRF, see Figure 2. A monochromatic X-ray beam at an energy of 15 keV ($\lambda = 0.83$ Å) was generated by an undulator and selected by a Si (111) double bounce monochromator. The condensing system comprised 5 200 μm-radius Be-lenses located 20 m from the source followed by a set of slits to restrict the beam size to 200×400 μm^2 and a 1D silicon compound refractive lens with 40 50 μm-radius lenslets located 55 m from the source. This produced a line beam of 200 nm in height and 200

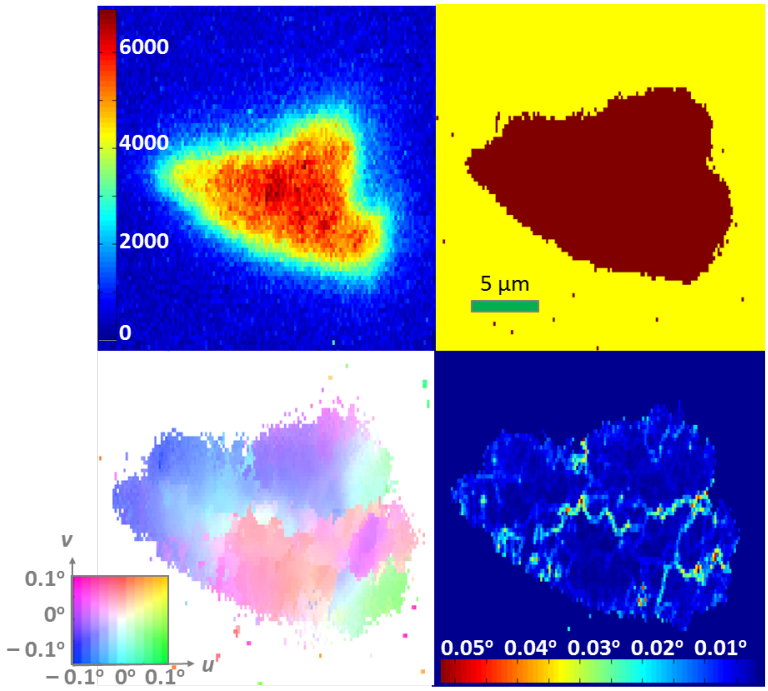

Figure 4. Preliminary data. The data shown is for a single layer of an approximately $15\times20\times20$ μm^3 recrystallizing grain. (a) Adding images for all measured tilts (u, v) gives a measure of the spatial distribution of total intensity, shown here in arbitrary units. (b) Setting a threshold for the total intensity gives an estimate of the grain shape on the micrometre-scale. (c) Colour-coding each pixel by the center position of the peak in the 2D rocking curve gives a map of the distribution of orientations. (d) The difference in orientation of neighbouring pixels gives an impression of very low angle boundaries within the grain.

μm wide, allowing us to illuminate one slice of the sample at a time with sufficient sampling statistics to capture images in 3-5 seconds. The objective consists of 72 50 μm-radius Be-lenses, which ultimately provided a magnification of 18 times over the 5.5 m sample-to-detector distance. The far-field detector was a FReLoN CCD detector with 2048 × 2048-pixels with an effective pixel size of 1.2 μm. The spatial resolution was thus limited by the optical performance of the objective lens, which is still better than 200 nm.

Images were collected for small tilts in the two perpendicular angles (u, v), see Figure 1. Both tilt-series covered $\pm0.1^{\circ}$, in steps of 0.005° for angle u along the θ-direction and in steps of 0.02° for the perpendicular angle v.

3.3. Results

From the total intensity of each image with different values of the tilts (u, v) a summed 2D rocking curve was obtained, see Figure 3. The two distinct peaks observed here indicate that at least two different orientations are present inside the grain. Adding all images gives an estimate of the grain morphology, see Figure 4(a) and setting an intensity threshold as in Figure 4(b) gives a measure of the grain shape, allowing us to compare grain shapes for example before and after annealing. 2D rocking curves for each pixel were constructed from the intensity of a single pixel in each of the 451 images. The lattice orientation associated with each pixel was determined as (u, v) of the maximum intensity in the 2D rocking curve. This is summarized

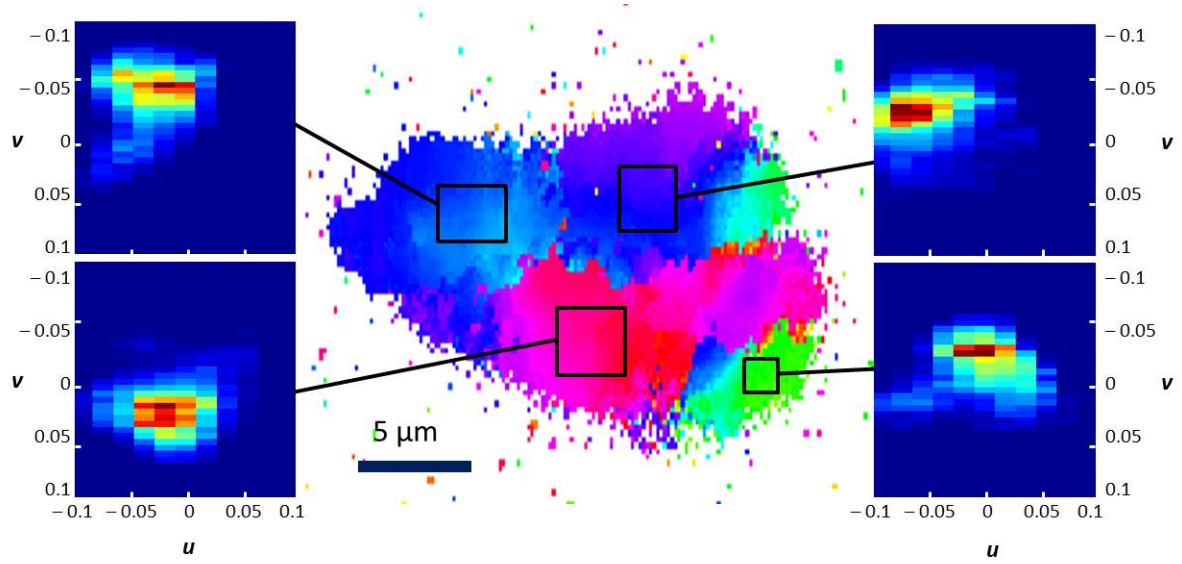

Figure 5. 2D Rocking curves of regions with slightly different orientation. Central image shows the recrystallizing grain colour-coded according to the lattice orientation. Insets show the 2D rocking curves in (u, v) of the marked regions.

in the colour-coded image in Figure 4(c). The difference in orientation between neighbouring pixels is shown in Figure 4(d).

Interestingly, the grain is observed to be subdivided by several very low angle boundaries separating regions of slightly different lattice plane orientations. These regions are $2-5$ μm across and their orientational differences are of the order of 0.1° or less as seen in the 2D rocking curves for different regions in Figure 5. The very low angle boundaries of 0.1° angular difference correspond to about $4 \cdot 10^6$ dislocations/m or a distance of more than 0.2 μm between dislocations. The internal structure of the recrystallizing grain may be due to the impurities present in Al1050 or be reminiscent of the deformed structure since the features are of similar size [10]. Note that the apparent sharpness of the very low angle boundaries in Figure 4(d) may be an artefact of the reconstruction process. Therefore, a thorough analysis of the image registration is necessary before further interpretation and characterization of these boundaries can be conducted.

The conclusion holds, however, that within a recrystallizing grain in the present sample there exist very low angle boundaries with 0.2 μm or longer between dislocations. This is at the limit of the current instrumental resolution, but in the near future we hope to increase the spatial resolution to about 50 nm. This will enable us to investigate in detail the very low angle subdivision of the recrystallizing grain and the strain fields associated with these internal boundaries. Further potential studies include *in situ* annealing and characterization of such recrystallizing grains to make films of the growth of recrystallizing grains and the possible changes within the grains, as well as characterization of the surroundings of the grains, deformed material or other grains.

4. Conclusion

We have demonstrated that Dark Field X-Ray Microscopy is a promising technique for studying polycrystalline materials in 3D. The technique offers relatively fast data acquisition and involves a hard X-ray line beam 200 nm in height and a set of X-ray lenses that magnifies the diffracted

signal. This setup allows us to non-destructively construct 3D maps of orientation and strain of micrometre-sized structures embedded in mm-sized samples of the same material with an angular resolution of about 0.005^{o} and spatial resolution of 0.2 μm, thereby providing a significant step forward for 3D materials characterization techniques.

Acknowledgments
The authors are grateful to W. Pantleon, S. Schmidt and C. Detlefs for scientific advice, ESRF for providing beamtime and the Danish Instrumentation Centre, Danscatt. The work is part of an ERC grant "diffraction based x-ray transmission microscopy".

References

[1] Schwartz A J, Kumar M, Adams B L and Field D P 2009 *Electron Backscatter Diffraction in Materials Science* (Berlin: Springer)
[2] Williams D B and Carter C B 2009 *Transmission Electron Microscopy: A Textbook for Materials Science* (Berlin: Springer)
[3] Poulsen H F 2004 *Three-Dimensional X-Ray Diffraction Microscopy: Mapping Polycrystals and their Dynamics* (Berlin: Springer)
[4] Ludwig W, Reischig P, King A, Herbig M, Lauridsen E M, Johnson G, Marrow T J and Buffire J-Y 2009 *Rev. Sci. Instrum.* **80** 033905
[5] Larson B C, Yang W, Ice G E, Budai J D and Tischler J Z 2002 *Nature* **415** 887
[6] Simons H, King A, Ludwig W, Detlefs C, Pantleon W, Schmidt S, Stöhr F, Snigireva I, Snigirev A and Poulsen H F 2015 *Nature Comm.* **6** 6098
[7] Hu H 1962 *Trans. Met. Soc. AIME* **224** 75
[8] Tanner B K 1976 *X-Ray Diffraction Topography* (Oxford: Pergamon Press)
[9] Snigirev A, Kohn V, Snigireva I and Lengeler B 1996 *Nature* **384** 49
[10] Hansen N and Juul Jensen D 2011 *Materials Science and Technology* **27** 1229